October 1984 LRP 252/84

TCA Papers
presented at

4th International Symposium on Heating
in Toroidal Plasmas
Rome, Italy, 1984

DISCONTINUOUS HEATING BEHAVIOUR OBSERVED IN THE TCA TOKAMAK AND ITS INTERPRETATION IN TERMS OF THE ALFVEN WAVE SPECTRUM

ALFVEN WAVE HEATING ON TCA

ALFVEN WAVE HEATING RESULTS IN TCA USING COATED BAR ANTENNAE

NON-LINEAR ANTENNA LOADING MEASUREMENTS IN TCA

DISCONTINUOUS HEATING BEHAVIOUR OBSERVED IN THE TCA TOKAMAK AND ITS INTERPRETATION IN TERMS OF THE ALFVEN WAVE SPECTRUM

K. Appert, A. de Chambrier, G.A. Collins, P.-A. Duperrex, A. Heym, F. Hofmann, Ch. Hollenstein, B. Joye, R. Keller, A. Lietti, J.B. Lister, F.B. Marcus, J.-M. Moret, S. Nowak+, A. Pochelon and W. Simm

Centre de Recherches en Physique des Plasmas
Association Euratom - Confédération Suisse
Ecole Polytechnique Fédérale de Lausanne
21, Av. des Bains, CH-1007 Lausanne/Switzerland

+ University of Fribourg, Switzerland

Introduction : Since Alfvén wave heating relies on the absorption of a wave's energy at resonance surfaces within the plasma, there should be some correlation between the observed heating and the position of these surfaces. The early heating experiments on TCA, while showing significant electron and ion temperature increases [1], failed to show such a correlation. Improvements to the experiment, particularly due to active current control and attempts to find the best limiter material and design, allowed confirmation of both the electron and the ion heating and increased the maximum rf power that could be delivered [2]. However, even with the cleaner experiment, there had been very little experimental evidence to relate the macroscopic plasma parameters to either the antenna excitation structure or the position in the Alfvén wave spectrum.

Recently, one striking exception has been found [2]. During a heating pulse in conditions which excite a resonance surface in the outer half of the plasma, a sharp discontinuity was observed in many of the plasma parameters. This feature occurs when a new mode appears in the spectrum and hence presumably the energy deposition profile is changed. The interest in this mode is not just because its appearance has such a dramatic effect on the heating behaviour, mainly by a reduction in the rate of electron density increase,

but also because it was not predicted by any of the theoretical calculations of the Alfvén wave spectrum. A tentative characterisation of the new feature [2] as a poloidally symmetric mode excited via toroidal coupling was made, and we have continued attempts to identify it and hence understand the reasons for its effect.

These attempts, as described in this paper, have followed two directions. Firstly detailed experiments and analyses have been performed to determine which antenna structures can excite the mode and to quantify the effects of heating both with and without the mode in the plasma. Secondly we have used a modified version of the ERATO stability code to give a two dimensional model of the excitation process [3], with the restriction of ideal MHD that $\omega/\omega_{ci} = 0$. We have been able to confirm our earlier identification of the new mode, and to show that it is due to toroidal coupling of different poloidal modes in the plasma.

The Alfvén wave spectrum in cylindrical and toroidal geometry : In cylindrical geometry it is possible to define an ideal antenna - one that excites a single resonance surface well-positioned within the plasma. In Fig. 1(a) measurements of the loading of the usual TCA antenna (N=2, M=1) are compared with a calculation that sums the contributions of several ideal cylindrical antennae [4]. The assumed positions of the principal resonance surfaces (n=±2, m=±1) are shown in Fig. 1(b).

The most obvious discrepancy between the measured and calculated curves in Fig. 1(a) is the appearance of a new mode near $\bar{n}_e = 3.2 \times 10^{19}$ m^{-3}. As seen in Fig. 1(b) this is at the threshold of the n=2, m=0 continuum. It is this mode that has the dramatic effect on plasma parameters during heating experiments and its excitation was not forseen for two reasons. Firstly our antenna has only parasitic m=0 component, and secondly in cylindrical geometry it is extremely difficult to couple energy to the m=0 resonance surface since no m=0 fast wave can propagate at this frequency. In addition an m=0 global eigenmode is not expected since magnetic field curvature, which assists in the formation of global eigenmodes [5], has only a small effect on m=0 waves.

To verify that the new mode is actually a result of the N=2, M=1 antenna configuration we have tried to excite it with all our available antenna phasings. The results are shown in Fig. 2. With N=1, M=1 the n=1, m=1 global eigenmode is clearly seen at $\bar{n}_e = 2.6 \times 10^{19}$ m^{-3} but is distinct from the global eigenmode of the new mode at $\bar{n}_e = 3.2 \times 10^{19}$ m^{-3}. This is particular-

ly obvious with an antenna phasing that produces an equal mixture of N=1 and N=2, when both peaks are visible. For all other antennae, no structure is seen in the spectra, particularly for N=2, M=0 which does not couple to the new mode. It is necessary to turn to toroidal geometry to predict the excitation of the new mode.

The most important effect of toroidicity is the coupling it induces between waves of different poloidal wavenumbers. In other words, an antenna designed to excite one resonance surface will also deposit energy into surfaces at different radii. The calculated positions of the resonance surfaces in toroidal geometry are shown in Fig. 1(b) for n=2. The surfaces are only slightly shifted with respect to their positions in the cylindrical model, and it is only at very low densities that a gap appears due to the coupling of pairs of poloidal modes near rational q-surfaces [6].

Although an ideal antenna does not exist in toroidal geometry it is possible to maximize the energy coupled to the desired resonance surface and reduce that lost to the edge modes. This has been achieved by weighting the current distribution to the interior of the torus, and gives a clearer picture of toroidal effects than that obtained in the previous study [3].

The TCA antenna always excites both $m=\pm 1$, so it is necessary to sum the contributions of two idealized M=+1 and M=-1 antennae. This minimizes the problems found previously [3] when trying to model an antenna of double helicity. In Fig. 3, the radial profiles of energy flux are shown for various positions in the spectrum. It is obvious that energy can be very efficiently coupled to the m=0 surface, with nearly 50 % of the total being absorbed near this surface when it is at mid-radius.

This has important repercussions for our heating experiments in that it provides a means for energy to be coupled into the interior of the plasma in a region of the spectrum which would otherwise be conducive to edge heating. In fact the majority of our heating experiments have been performed in this region, and it is due to the toroidal coupling to the m=0 surface that we have been able to get energy into the centre. In the theoretical studies we have also found evidence of the m=0 global eigenmode near $\bar{n}_e = 3.1 \times 10^{19}$ m^{-3} and so we are now confident that the new mode can be identified as n=2, m=0.

Experimental Observations of the Discontinuous Behaviour : The clearest way to observe a change in the macroscopic plasma parameters as a result of a change in the energy deposition profile is to move through the spectrum du-

ring a heating pulse. This is unavoidable on TCA since the plasma density is observed to increase with the introduction of rf power. Fig. 4 shows a typical shot in which the density increases to cross into the continuum of the n=2, m=0 mode. The peak in loading caused by the m=0 global eigenmode passes without much change in the macroscopic parameters, but the onset of the continuum has a dramatic effect. Most importantly there is a break in the density rise which leads to a maximum in the soft X-ray flux and $\beta + l_i/2$. After the discontinuity there is an increase in the H_α radiation which normally decreases upon introduction of the rf power. The radiated power intensity as measured by the bolometer also undergoes a change at the discontinuity giving a reduced rate of rise despite an increase in the total rf power coupled to the plasma.

Magnetic field probes in the shadow of the limiter are particularly helpful in detecting the presence of the global eigenmode. These measurements, shown in Fig. 4, can also help in the identification of the mode since the components of the rf field in the vacuum satisfy the relation $\left|\frac{b_\phi}{b_\theta}\right| = \frac{n}{m}\frac{r}{R}$. The peak is mostly evident on the b_ϕ probe, confirming its identification as an m=0 global eigenmode.

Both the measurements of ion temperature (neutral particle analyser) and electron temperature (soft X-ray diodes) also show the discontinuity, but it is possible to interpret their change as a direct result of the break in the density increase. At present our experiment is still not clear enough to give a fair comparison between heating above and below the discontinuity except that the density rise is less above. Measurements of the electron density profile with an 8-channel FIR interferometer show that the density increase is greatest near the edge of the plasma. Even though the central density also increases, the profile becomes quite flat just before the n=2, m=0 continuum but starts to peak again after the discontinuity. This observation helps to confirm that a change has indeed occured in the energy deposition profile.

Recently a similar discontinuity has been observed crossing into the n=2, m=1 continuum at $\bar{n}_e = 7.3 \times 10^{19}$ m^{-3}. Previously this had not been so clear due to less well-controlled operation in the higher density range. Also crossing into a new continuum has often been associated with the onset of mode-dominated discharges thought to be caused by a change in current profile as a result of the change in energy deposition profile. Unfortunately this can either lead to a disruption (as is often the case at the higher density of the n=2, m=1 mode) or a loss of plasma current control and thus a saturation of the density increase. This latter effect actually accentuates the

discontinuous behaviour and assisted in its initial observation.

Conclusion : We have found that our N=2, M=1 antenna can couple efficiently to the n=2, m=0 resonance surface as a result of toroidicity. This helps to deposit energy towards the centre of the discharge and the appearance of this surface in the plasma can be seen as a discontinuity on many of the macroscopic parameters. Without understanding the mechanism for the electron density increase it is difficult to explain the discontinuity except that it provides evidence of a connection between observed plasma behaviour and the Alfvén wave spectrum.

Acknowledgements : We would like to thank the TCA support team without whom none of our experimental work would be possible. The work was partially supported by the Swiss National Science Foundation.

References :

[1] de CHAMBRIER A. et al., Plasma Phys., 25 (1983) 1021
[2] BEHN R. et al., Plasma Phys. Contr. Fusion, 26 (1984) 1A, 173
[3] APPERT K. et al., Nucl. Fusion, 22 (1982) 903
[4] APPERT K. and VACLAVIK J., Plasma Phys., 25 (1983) 551
[5] APPERT K. et al., Plasma Phys., 24 (1982) 1147
[6] KIERAS C.E. and TATARONIS J.A., J. Plasma Phys., 28 (1982) 395

Keywords : Alfvén wave heating, TCA, toroidal effects.

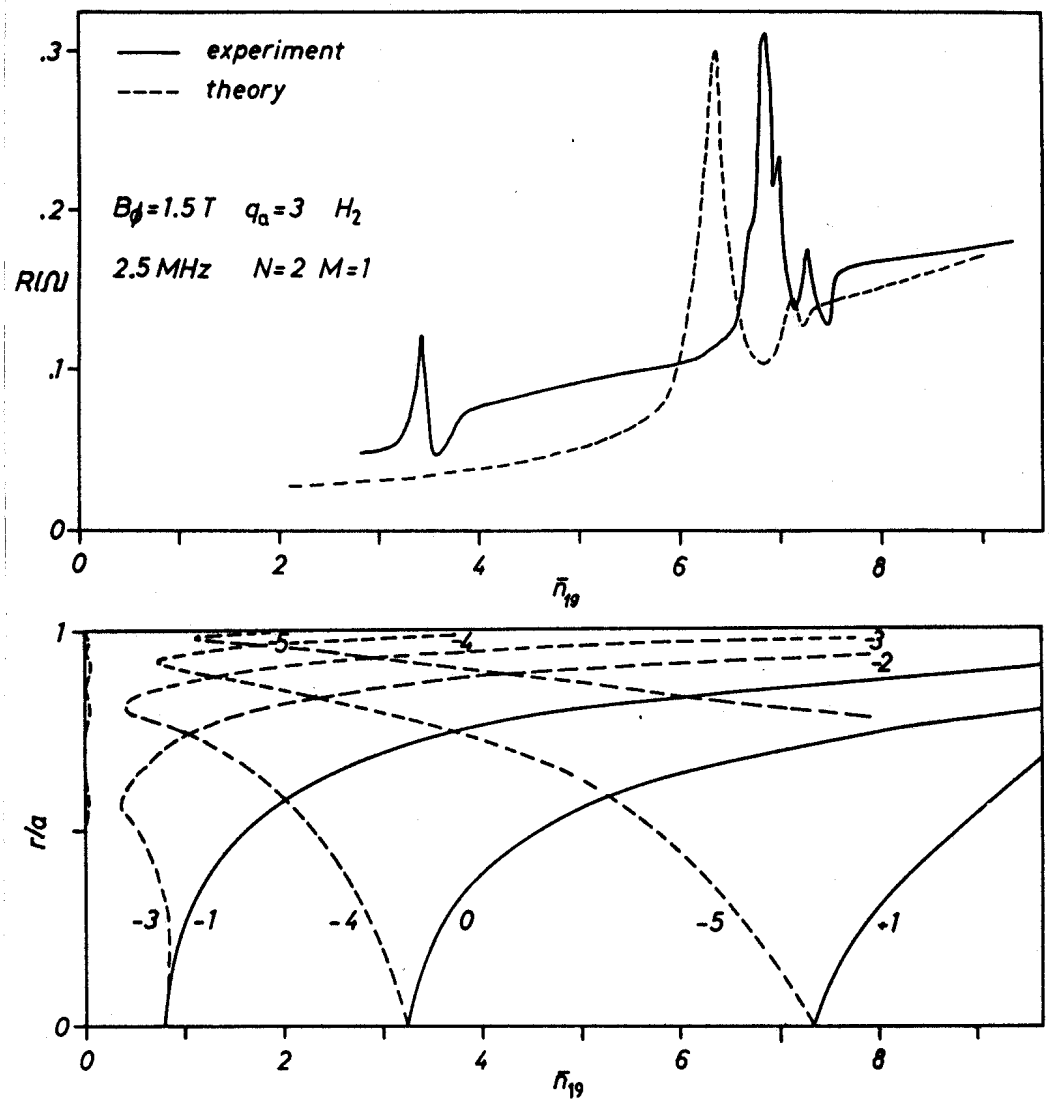

Figure 1: (a)Measured and calculated antenna loading spectrum for typical TCA parameters. (b)Positions of the resonance surfaces in toroidal geometry, labelled by their dominant poloidal wavenumber. The principal surfaces (m=-1,0,+1) are only slightly shifted inwards from their 'cylindrical' positions.

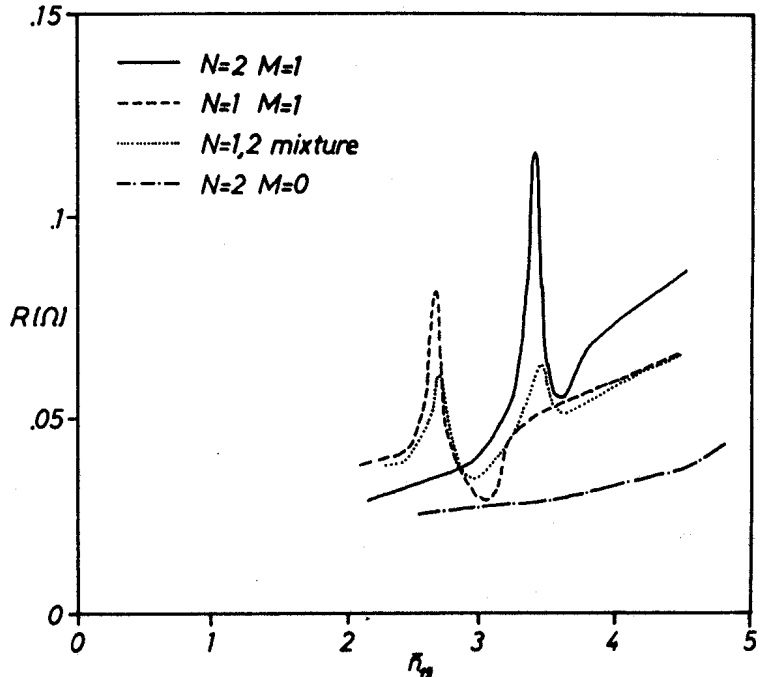

Figure 2: Loading measured for different antenna phasings. Both the peak of the n=1,m=1 global eigenmode and the new mode (n=2,m=0) can be seen.

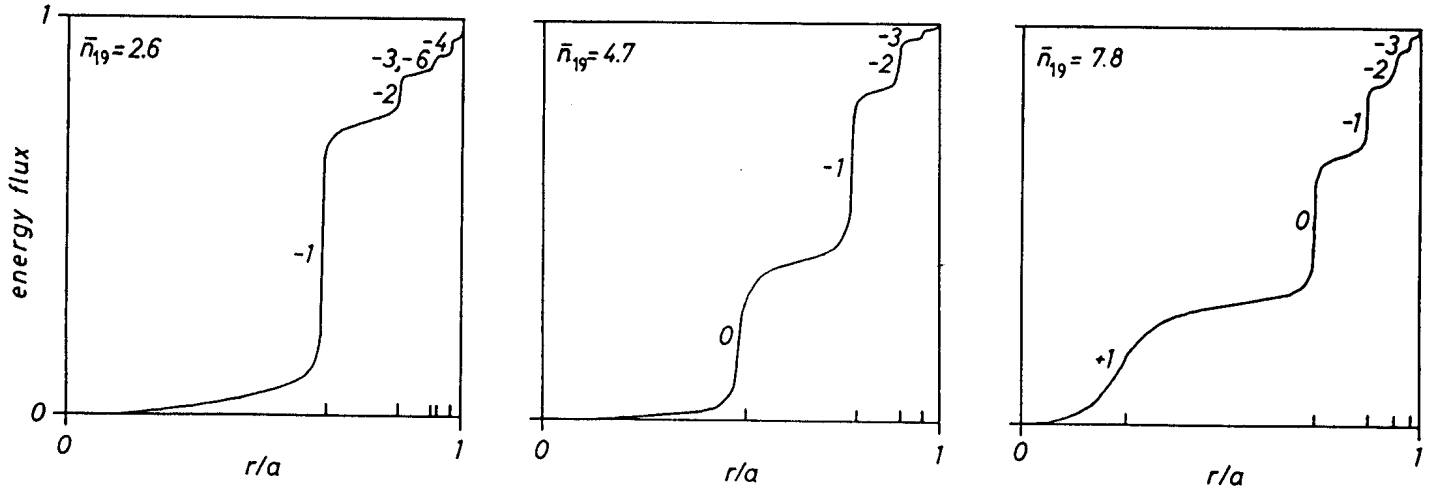

Figure 3: Radial profiles of energy flux for three positions in the spectrum for an N=2,M=1 antenna. The positions of the important resonance surfaces are marked. Note good coupling to the interior by the m=0 surface.

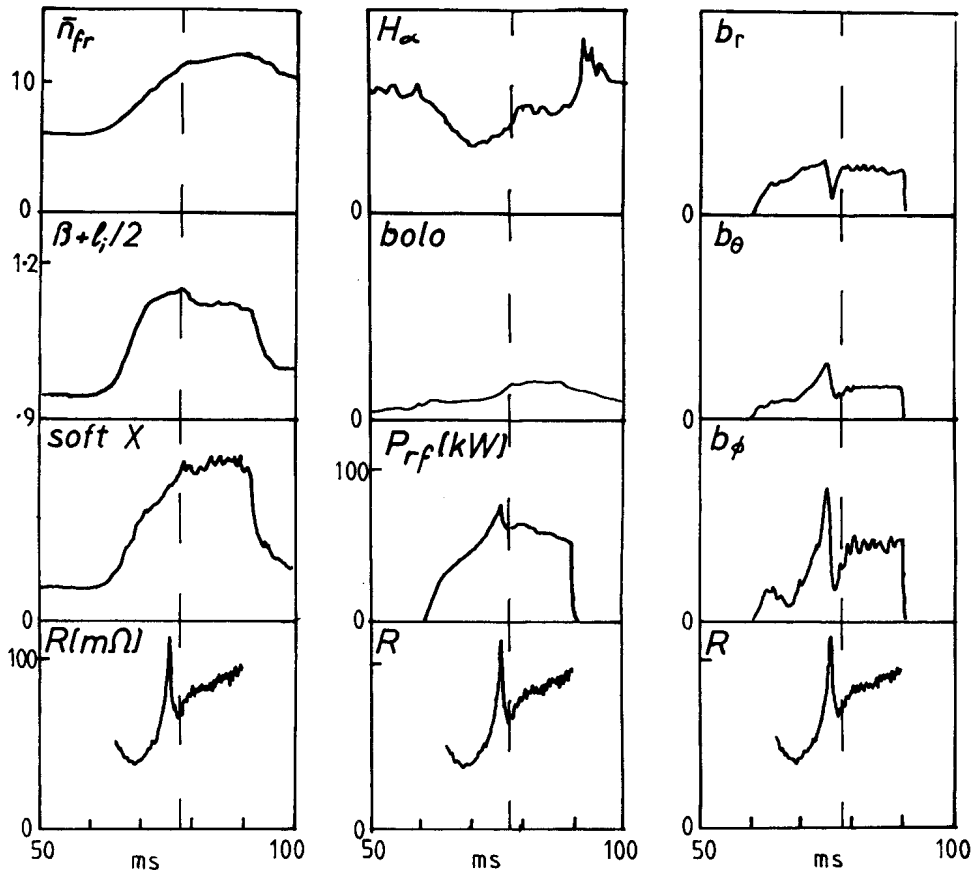

Figure 4: A typical TCA shot which crosses into the n=2,m=0 continuum. The discontinuity is seen on many of the plasma parameters. The wavefield probes and antenna loading assist in determining the position in the spectrum

ALFVEN WAVE HEATING ON TCA

A. de Chambrier, G.A. Collins, P.-A. Duperrex, A. Heym, F. Hofmann, Ch. Hollenstein, B. Joye, R. Keller, A. Lietti, J.B. Lister, F.B. Marcus, J.-M. Moret, S. Nowak*, A. Pochelon, W. Simm and S. Veprek**

Centre de Recherches en Physique des Plasmas
Association Euratom - Confédération Suisse
Ecole Polytechnique Fédérale de Lausanne
21, Av. des Bains, CH-1007 Lausanne/Switzerland

* University of Fribourg, Plasma Physics Department,
CH-1700 Fribourg/Switzerland

** Institue of Inorganic Chemistry, University of Zurich,
CH-8057 Zürich/Switzerland

Abstract

Recent results of Alfvén wave heating in the TCA Tokamak are briefly reviewed. Measurements of the electron temperature and electron density in the TCA scrape-off layer during high power RF heating are presented in detail. It is found that antenna-plasma interaction may lead to a non-Maxwellian edge plasma. Its impact on the interpretation of the edge measurements and the antenna and screen design are discussed.

Keywords: Tokamak device, radio frequency heating, Alfvén wave heating, edge measurements, TCA.

Introduction

Alfvén resonance absorption below the ion cyclotron frequency as a plasma heating method is being studied on the TCA Tokamak at Lausanne /1/. Since the early days of operation, a stainless steel modular RF antenna structure has been used /2/. A large radiative power loss from the plasma was observed during RF heating, and was progressively reduced by the appropriate choice of limiter material and limiter shape /3/. Recently, over 200 kW of RF power have been delivered to the plasma, resulting in significant electron and ion heating /4/. Measurements of the edge plasma behaviour seem to show evidence of an increased electron temperature /5/ such as reported for other RF heating schemes /6/. The electron density, however, is observed to decrease during the RF pulse. Most recently, newly designed bar antenna with TiN-coating have been mounted in TCA /7/.

In this paper, we first give a summary of the recent heating results. This is followed by a short discussion of the results of surface studies on the stainless steel antenna. Detailed measurements of the TCA scrape-off layer during high power RF heating are presented. Finally, the impact of these measurements on future RF antenna and shield design and on the physics of the scrape-off layer during intense RF heating is discussed.

Experimental Parameters

The main operating parameters of the TCA Tokamak are $R = 0{,}61$ m, $a = 0{,}18$ m, $B_\phi \leq 1{,}5$ kG, $I_p \leq 170$ kA /1,4/. The experiments were carried out mainly in deuterium. The material of the limiter for the present studies was carbon.

The original RF antenna structure shown in Fig. 1 is one of eight groups sited at four different toroidal locations. The antenna material is stainless steel (316 LN). The whole RF structure is located 2 cm behind the limiter. The antenna surface represents about 16 % of the plasma surface area. Figure 2 shows the new bar antenna installed in TCA. This antenna is manufactured out of 1 cm diameter stainless steel bars. The polished antenna was finally coated with TiN using the CVD process. The thickness of the coating is about 6 μ. The limiter-antenna distance has been increased to 3 cm.

In all the experiments presented here no antenna screens were used. For both sets of antennae, each of the eight groups is electrically floating with respect to the vacuum chamber. Additional circuitry permits a negative polarization of the whole antenna up to -400 V in vacuum. The type of excitation can be chosen by individual phasing of the different antenna groups. The antenna frequency for the data presented here is 2.5 MHz.

Heating results

The heating results were carried out mainly in deuterium at 15 kG and with plasma currents up to 122 kA ($q_I \sim 3,3$). Over 200 kW of RF power have been delivered to the plasma without causing disruptions. This RF power is roughly equal to the ohmic heating power. Figure 3 shows the waveforms for a discharge with 130 kW of RF power input /4/. The central plasma density chosen during the RF pulse was $3 - 5 \times 10^{13}$ cm^{-3} in order to be below the (n,m) = (-2,-1) discrete Alfvén wave resonance. The RF pulse is accompanied by an increase of the line-averaged density. The electron temperature increase was maintained far longer than was previously the case. The increase of the electron temperature remained roughly linear with delivered power and an incremental heating factor of $n_e \Delta T_{eo}/P_{RF} = 3.4 \times 10^{13}$ eV/cm^{3}kW is obtained. Under standard conditions the central ion temperature increases from $T_{io} \approx 250$ eV to ≈ 430 eV with 140 kW of RF power input. A heating factor value of $n_e \Delta T_{io}/P_{RF} = 1.5 \times 10^{13}$ eV/cm^3 kW is found. Considerable effort has been made to reduce the radiation power losses during RF. Different limiter shapes and limiter materials (stainless steel, carbon, TiC-coated carbon) reduced the radiation power losses from 2.6 W/cm^3 to 0.6 W/cm^3 during 80 kW RF pulses. Vacuum UV spectroscopic measurements revealed an increase in metallic impurities. The stainless steel plate antenna with its large surface area near the plasma has been suspected to be the most probable source of such impurities. With the new TiN-coated bar antenna the metallic impurities in the centre of the plasma have been strongly reduced.

Surface study of the stainless steel antenna

The stainless steel antennae have been used since the beginning of TCA operation in 1980. At the end of 1983, they were replaced by TiN-coated bar antennae. Inspection of the stainless steel antenna plates after dismantling showed a considerable number of arc traces. The highest arc density was found on the bottom antenna groups. No recent evidence is available to determine whether or not the arcing occurred preferentially during the RF phase. Previous observations of the antenna group with the aid of a high speed camera indicated no arcing during RF.

Inspection with an optical microscope revealed that melting occured at the leading edges of the antenna plates. In general only the edges of the outermost antenna plate have been affected, especially the edges on the ion side.

To study impurity fluxes onto the antenna plates, Molybdenum samples were attached to them. The samples were oriented either perpendicular or parallel to the antenna plate. The surfaces of these samples have been analysed by means of XPS (X-ray photoelectron spectroscopy). The main impurities discovered on these samples are carbon, iron and oxygen. On the sample surface which was oriented parallel to the antenna plate, much less impurities have been found compared with the impurity concentration found on the sample oriented perpendicular to the antenna plate. This suggests either sputtering on the antenna surface or a low impurity flux in this direction. Further Molybdenum samples coated with a thin layer of gold are presently positioned on the bar antennae in order to determine whether sputtering is important.

Scrape-off layer measurements

A single movable Langmuir probe has been used to measure the electron density and electron temperature in the scrape-off layer. The Langmuir probe is located in the equatorial plane, between two groups of antennae and approximately opposite the limiters. The electron temperature was obtained from analysis of the Langmuir probe characteristic. This analysis was performed by assuming that the plasma were Maxwellian. Hot electron populations due to strong antenna-plasma interaction can complicate this analysis, as we shall

show. The ion density was evaluated from the ion saturation current. The ion saturation current was measured at a typical probe bias of -200 V. The perpendicular ion temperature in the edge plasma was obtained from a Katsumata probe /8/. This probe was fixed at 4 cm behind the limter radius.

Figure 4 shows the electron temperature profile in the scrape-off layer during RF heating experiments (P_{RF} = 100 kW) using the stainless steel plate antenna. When compared with the electron temperature during the ohmic heating phase a strong increase is observed /5/. Similar behaviour has been observed in ICRH experiments /6/. It is noticeable that the e-folding length λ_{Te} before and during the RF phase does not significantly change.

A completely different behaviour has been found for the electron density as shown in Fig. 5. The electron density drastically decreases during RF and the density profile e-folding length λ_{ni} increases. It is interesting to note that nearly flat density profiles were observed in the RF phase. Moreover, the decreasing density in the scrape-off layer seems to be consistent with the observed decrease in D_α emission during RF as reported earlier /4/.

Edge temperature profile measurements with the TiN-coated bar antenna are presented in Figs. 6 and 7. With this new antenna set an increase in the electron temperature is observed as in the previous case. The electron temperatures are comparable with the temperature with the plate antenna. However, it seems that in the region of the antenna position slighly higher temperatures are encountered. This may be explained by the fact that during the RF phase, due to antenna-plasma interaction, the electron distribution function becomes non-Maxwellian. The biggest difference is found in the behaviour of the electron density. In the case of the bar antenna, the density decrease during the RF phase is reduced. The large modification to the density profile in the edge-plasma, found with the plate antennae, has been considerably reduced with the bar antennae. A slight density dip in the antenna region cannot be excluded.

The power dependence of the electron temperature and electron density is shown in Figs. 8 and 9 for three different probe positions. The temperature shows no clear dependence on RF power. A much clearer dependence on RF power is found for the electron density and Fig. 9 shows that the electron densi-

ty at all probe positions studied decreases roughly linearly with RF power.

There is some evidence that the excitation mode or the wavefield magnitude influences the edge plasma considerably. In Fig. 10, time resolved electron temperatures are shown measured 1.25 cm behind the limiter. During the sweep through the (n,m) = (-2,-1) resonance peak, indicated by the b_ϕ component of the wavefield magnetic field, a strong temperature increase is seen. The ion saturation current as well as the D_α emission have not been influenced by the strong transient absorption. Particle confinement times calculated from the probe data /9/ tend to confirm the D_α measurements /4/, which indicated an increase of the confinement time.

The ion temperature in the edge plasma can be determined from different diagnostics. One of the easiest diagnostics is the so-called Katsumata probe. The measured perpendicular ion temperature obtained from a Katsumata probe on TCA is shown in Fig. 11. As already seen for the electron temperature an increase in the ion temperature is observed. The temporal behaviour of the edge ion temperature is very similar to the ion heating measured with the Neutral Particle Analyser.

Edge measurements have been made with electrical probes located in the scrape-off layer. All the measurements are time-averaged over many cycles and no RF timescale time-resolved measurements of the electron temperature and electron density are available yet. It is well known that probe measurements can be strongly affected by intense RF fields. Several different studies have been carried out on this subject /10,11/.

One recent study shows that in a large volume, low density plasma during intense RF, hot and cold electron distributions exist /12/. This electron beam, driven by the RF, may in fact lead to an important error of the plasma temperature measurements if it is not recognized and accounted for. A detailed check of the Langmuir characteristics indeed revealed that a hot electron population during RF may exist. Figure 12 shows the measured probe current before and during the RF pulse. This measurement shows a very different behaviour of the probe current during the ohmic heating phase and the RF phase. In Fig. 13 semi-logarithmic plots of the Langmuir characteristics

during lower RF power experiments are presented. In the ohmic heating phase, the straight line indicates that the edge plasma was Maxwellian. In the presence of RF, deviations from the straight line were observed. Under this condition, the edge plasma has to be considered to be non-Maxwellian even at low power. A careful analysis of the probe characteristics reveals that an electron beam with a beam energy of about 20 eV exists. This energy corresponds roughly to the antenna DC potential change, observed during the RF pulse at this low power. There are indications that the electron beam energy and beam density increase with RF power. However, additional measurements are necessary to verify this dependence. Also, large improvements in the time resolution of the probe measurements should be possible in the future, permitting the study of the formation and behaviour of the non-Maxwellian edge plasma during intense RF heating.

The presence of intense electron beams may not only lead to misinterpretation of the probe signals. The electron beam gives rise to an important self-polarisation of the whole antenna structure. Its presence may lead to large sheath potentials, not only of the antenna, but also of the limiters, therefore inducing arcing and sputtering. In particular, ions accelerated through many tens of volts become very efficient at sputtering. Also, direct electron bombardment may contribute to the heavy impurity flux. Furthermore, the electron beam may drive strong plasma instabilities in the scrape-off layer.

The following model is proposed to explain the antenna-plasma interaction. In TCA the antenna system is immersed in the edge plasma and the terminals of each antenna oscillate with an amplitude of about ± 200 V at 2,5 MHz. The antenna, therefore, acts as a large Langmuir probe. When a section of the antenna is biased positively, it draws the electron saturation current. Currents up to about 30 A/cm^2 have been estimated, which represents a considerable power loss. This effect appears as additional resistive loading of the antenna and could lead to arcing and melting. When the antenna region is biased negatively the plasma ions are accelerated onto the antenna and sputter very efficiently, leading to a large impurity flux into the plasma. This phenomenon may explain the observed strong plasma-antenna interaction at the antenna edges. Furthermore, this simple model is supported by high frequency measurements of the current flowing into a grounded Langmuir probe. With no plasma there was zero pick-up from the RF antennae. The RF

generator delivers a pure 2.5 MHz sine wave and the measurement is shown in Fig. 14. A superposition of 2.5 MHz and 5 MHz is evident. Current density oscillations of a few A/cm^2 are observed, indicating strong plasma-antenna interaction. The RF currents seem largest near the plasma and show a dip at the antenna radius. Spectral analysis of the probe signals show the presence of several higher harmonics of the driving frequency and also higher frequency noise.

Measurements of density fluctuations at the RF frequency are not yet really conclusive. In order to detect density fluctuations, the probe tip must be negatively biased and the probe signal may be perturbed by direct pick-up due to capacitive coupling between the probe-tip and the antenna system. Nevertheless, density fluctuations at the driving RF frequency were observed in spite of this pick-up.

In order to reduce the effects of the edge plasma on the antenna, we are planning to install lateral TiN-coated screens 5 cm from each side of each antenna group. Their main effect should be to reduce the electron density in the scrape-off layer behind the limiters and so reduce the above effects as much as possible.

In conclusion, we have shown that during Alfvén wave heating experiments, as in other RF schemes, the edge electron temperature apparently increases. However, this apparent temperature increase is possibly due to the effects of a non-Maxwellian plasma. The non-Maxwellian plasma is formed by the interaction of the RF field and the edge plasma. The present antenna structure can act as a large Langmuir probe. Intense currents and their associated polarisation may lead to impurity fluxes into the plasma. This effect may be reduced by adding lateral antenna screens.

Acknowledgements

We thank M. Marmillod and the TCA support team for their excellent support and Mr. Ripper for the construction of the probes. Also, the great encouragement from Prof. F. Troyon is highly recognized. The present work was partially supported by the Swiss National Science Foundation.

References

/1/ CHEETHAM, A.D., HEYM, A., HOFMANN, F., HRUSKA, K., KELLER, R., LIETTI, A., LISTER J.B., POCHELON A., RIPPER, H., SIMIK, A., and TUSZEL, A., 11th Symposium on Fusion Technology, Oxford, Vol. 1 (1980) 601.

/2/ DE CHAMBRIER, A., CHEETHAM, A.D., HEYM, A., HOFMANN, F., JOYE, B., KELLER, R., LIETTI, A., LISTER, J.B., POCHELON, A., SIMM, W., TONINATO, J.L., and TUSZEL, A. Proc. of the 3rd Joint Varenna-Grenoble International Symposium, Heating in Toroidal Plasma, Grenoble, Vol. II (1982) 1117.

/3/ BEHN, R., HOFMANN, F., HOLLENSTEIN, CH., JOYE, B., LISTER, J.B., NOWAK, S., O'ROURKE, J., POCHELON, A., PEACOCK, N.J., and STAMP, M.F., 11th European Conference on Controlled Fusion and Plasma Physics, Aachen, Vol. II, C28, (1983) 471.

/4/ BEHN, R., DE CHAMBRIER, A., COLLINS G.A., DUPERREX, P.A., HEYM, A., HOFMANN, F., HOLLENSTEIN, Ch., JOYE, B., KELLER, R., LIETTI, A., LISTER, J.B., MORET, J.M., NOWAK, S., O'ROURKE, J. POCHELON, A., and SIMM, W., Plasma Physics 26 (1984) 173.

/5/ HOFMANN, F., HOLLENSTEIN, CH., JOYE, B., LIETTI, A., LISTER, J.B., POCHELON, A., and VEPREK, S., accepted for publication in J. Nucl. Matter (1984).

/6/ TFR Group, 11th European Conference on Controlled Fusion and Plasma Physics, Aachen, Vol. II, C34 (1983) 493.

/7/ DE CHAMBRIER, A., COLLINS, G.A., DUPERREX, P.A., HEYM, A., HOFMANN, F., HOLLENSTEIN, CH., JOYE, B., KELLER, R., LIETTI, A., LISTER, J.B., MARCUS, F.B., MORET, J.-M., NOWAK, S., POCHELON, A., and SIMM, W., 4th Int. Symposium on Heating in Toroidal Plasmas, Rome, 1984.

/8/ ODAJIMA, K., KIMURA, H., MAEDA, H., and OHASA, K., Japan J. Appl. Physics 17 (1978) 1281.

/9/ STAIB, P., J. Nucl. Matter 111 & 112 (1982) 109.

/10/ BOSCHI, A., and MAGISTRELLI, F., Il Nuovo Cimento 29 (1963) 487.

/11/ CRAWFORD, F.W., J. Appl. Phys. 34 (1963) 1897.

/12/ SCHUMACHER, R.W. HERSHKOWITZ, N., and MacKENZIE, K.R., J. Appl. Phys. 47 (1976) 886.

Figure Captions

Fig. 1 Stainless steel plate antenna group.

Fig. 2 TiN-coated bar antenna.

Fig. 3 Typical waveforms (15 kG, D_2)

Fig. 4 Electron temperature profile

Fig. 5 a) Electron density profile (before and after the RF pulse) (stainless steel antenna)

b) Electron density profile (during the RF pulse) (stainless steel antenna)

Fig. 6 Electron temperature profile (TiN-coated antenna)

Fig. 7 Electron density profile (TiN-coated antenna)

Fig. 8 RF power dependence of the electron temperature at 3 different probe positions

Fig. 9 RF power dependence of the electron density at 3 different probe positions

Fig. 10 Time evolution of the electron temperature

Fig. 11 Edge ion temperature

Fig. 12 Langmuir probe characteristics

Fig. 13 Semi-logarithmic presentation of the Langmuir characteristics at low RF power

Fig. 14 RF currents on a grounded Langmuir probe

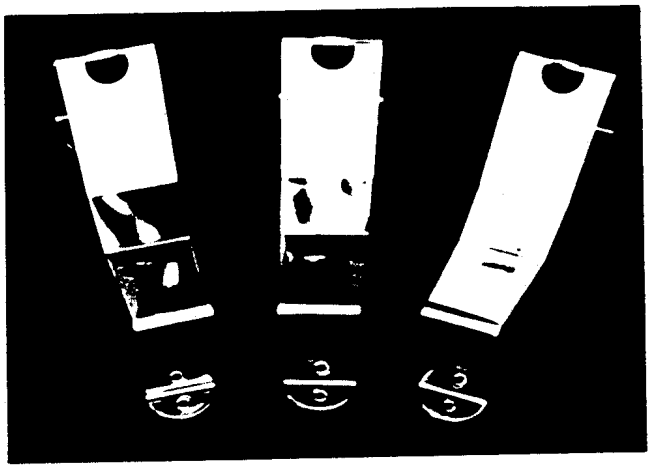

Fig. 1

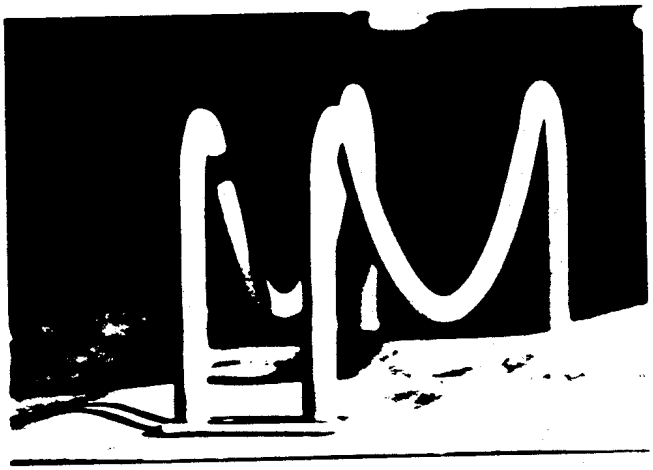

Fig. 2

Stainless steel antenna /Carbon limiters

14332,15kG;D_2,(N,M)=(2,1),Prf=130kW

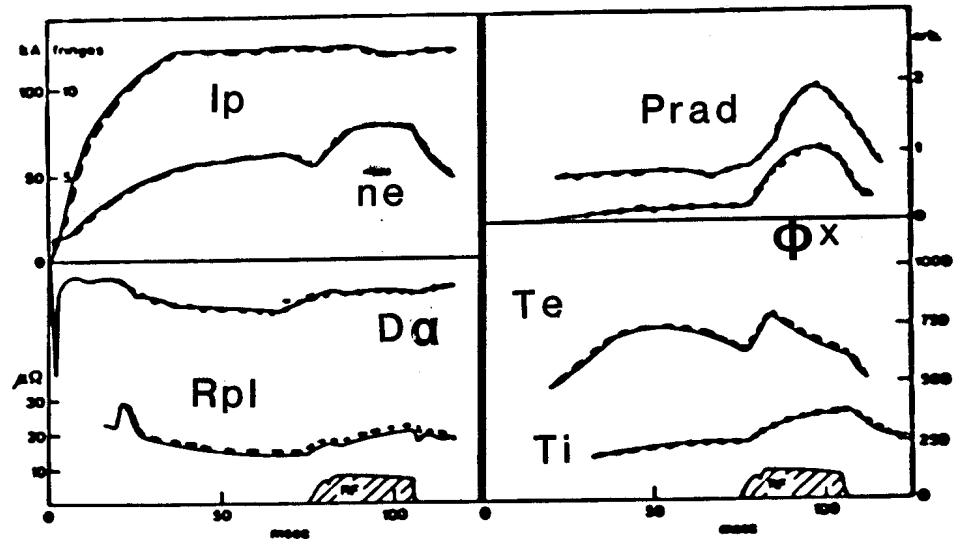

Fig. 3

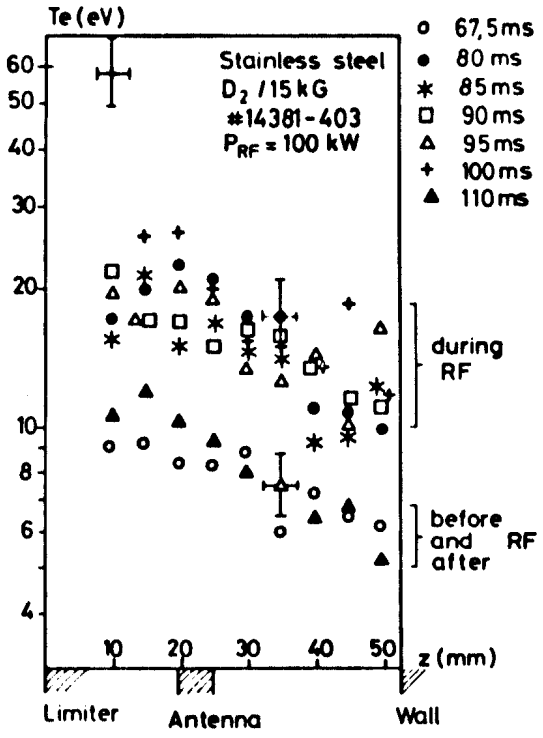

Fig. 4

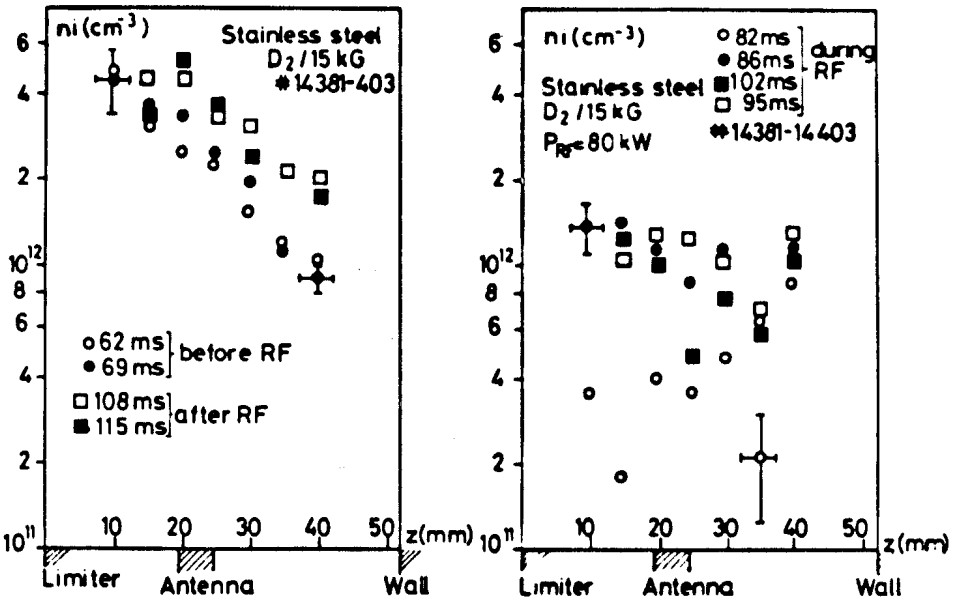

Fig. 5

a)

b)

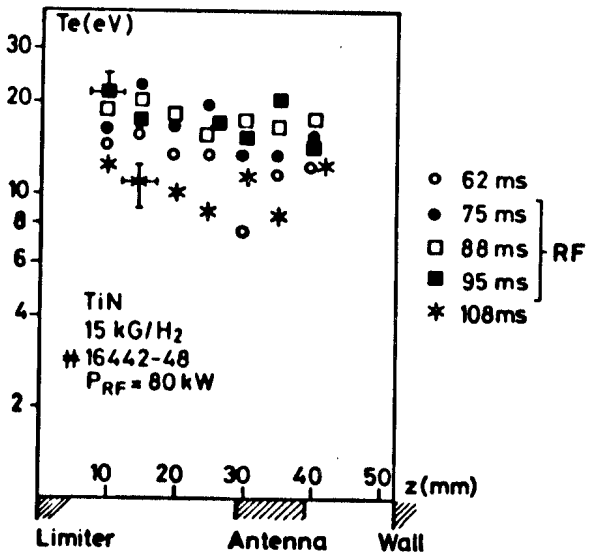

Fig. 6

Fig. 7

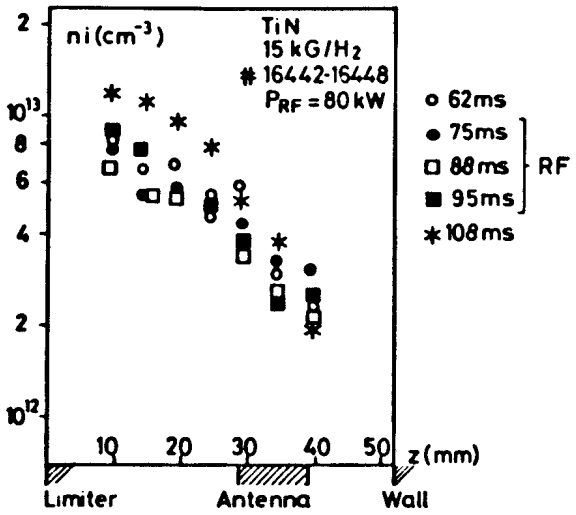

Fig. 8

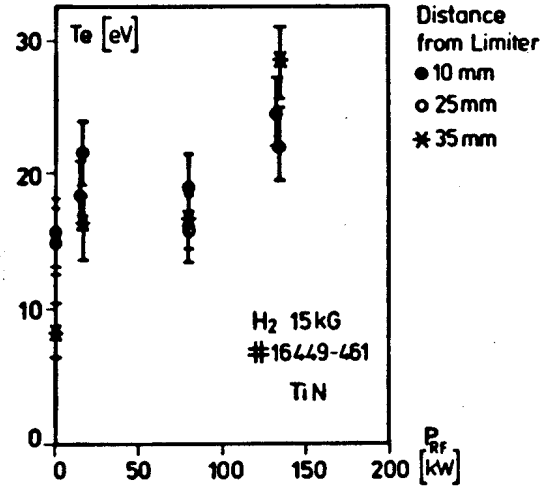

Fig. 9

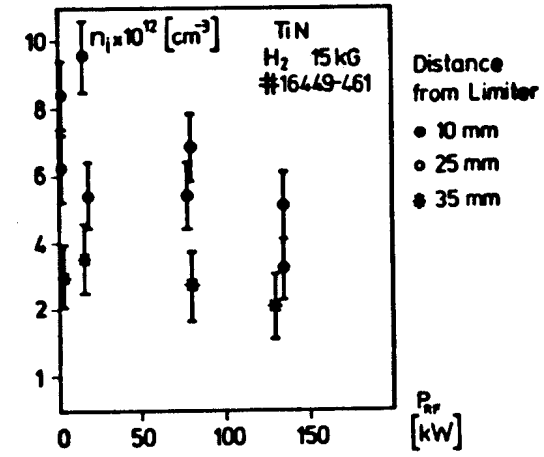

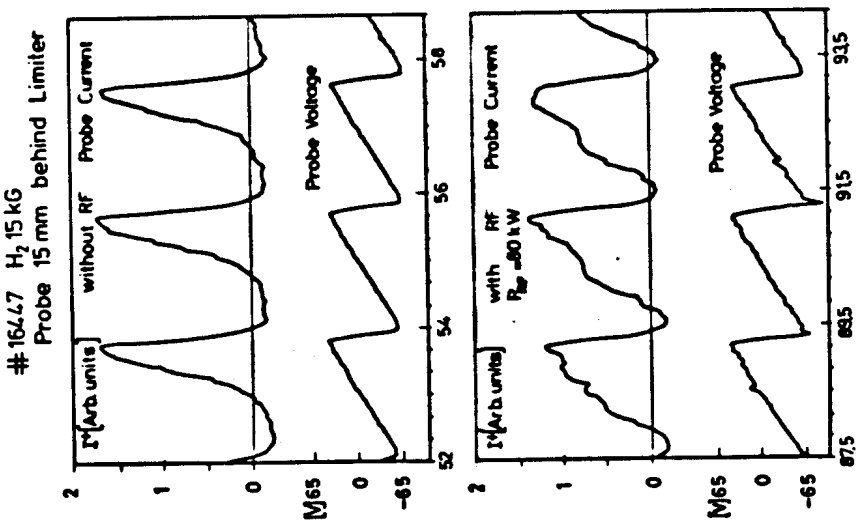

Fig. 12

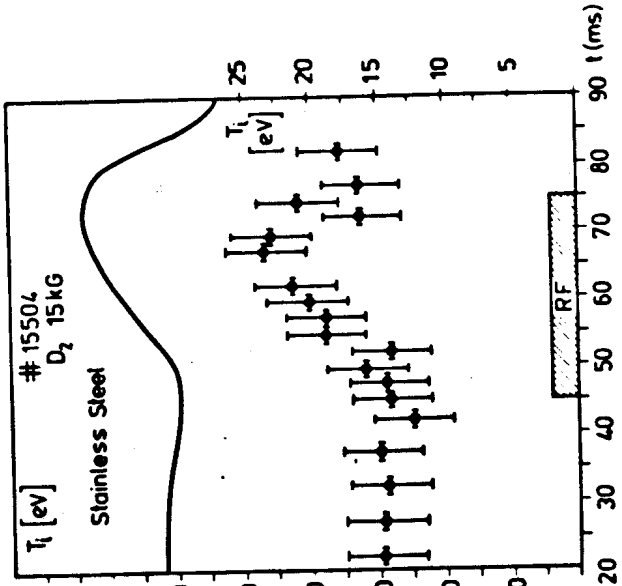

Fig. 11

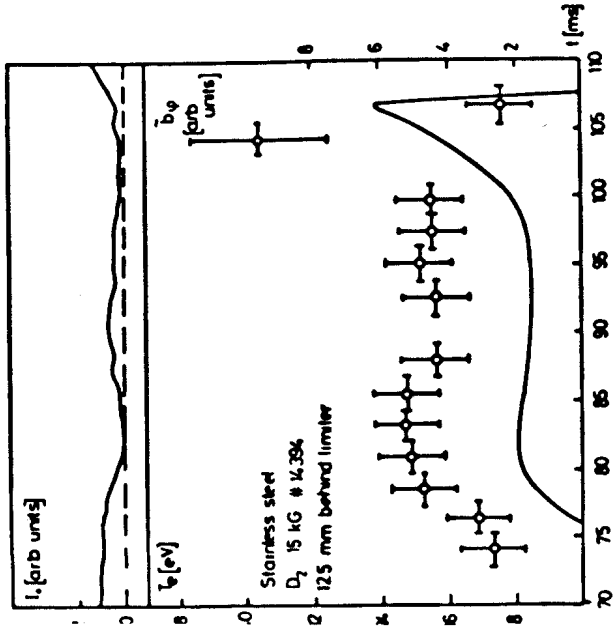

Fig. 10

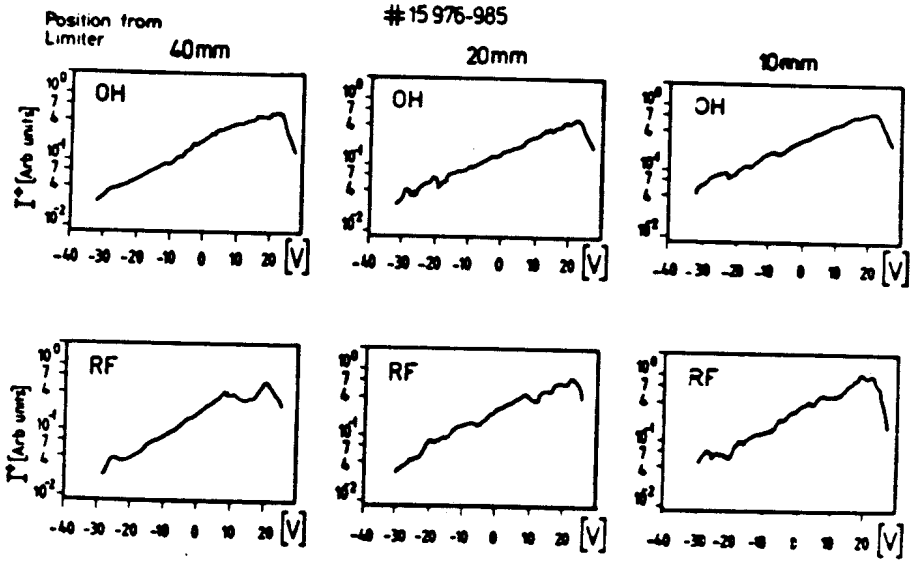

Fig. 13

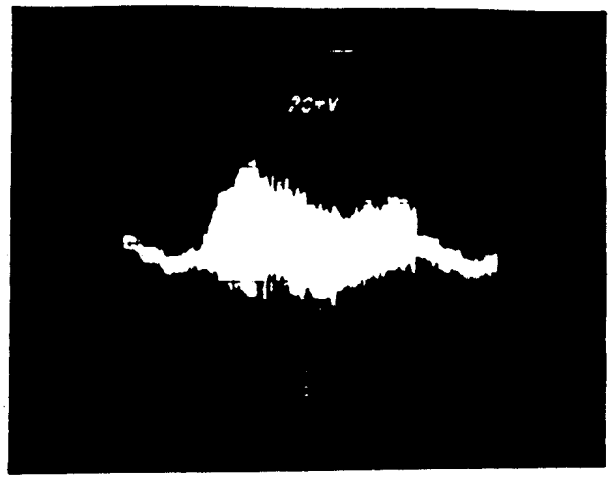

Shot 15912

(stainless steel)

Plasma side of antenna

x= 5 ms/div

y= 2A cm^{-2}/div

Fig. 14

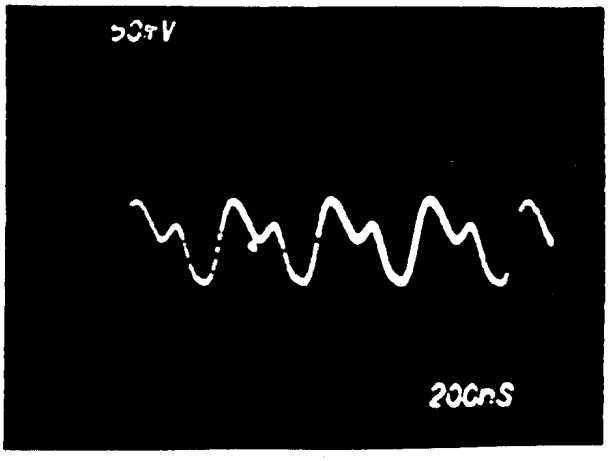

Shot 16402

(TiN)

at antenna position

x= 200 ns/div

y= 5A cm^{-2}/div

ALFVEN WAVE HEATING RESULTS IN TCA USING COATED BAR ANTENNAE

A. de Chambrier, G.A. Collins, P.-A. Duperrex, A. Heym, F. Hofmann, Ch. Hollenstein, B. Joye, R. Keller, A. Lietti, J.B. Lister, F.B. Marcus, J.-M. Moret, S. Nowak+, A. Pochelon and W. Simm

Centre de Recherches en Physique des Plasmas
Association Euratom - Confédération Suisse
Ecole Polytechnique Fédérale de Lausanne
21, Av. des Bains, CH-1007 Lausanne/Switzerland

+ University of Fribourg, Switzerland

Abstract : The Alfvén Wave launching antennae in TCA have been changed. The wide stainless steel plates previously used have been replaced by a simple bar-antenna structure which has nonetheless maintained a pure n-spectrum. The antennae have also been coated with titanium nitride. We present results on the coupling properties of the new antennae and their effects on the plasma. Preliminary indications are that there is a considerable reduction in the metallic impurity concentration following this change.

Introduction : The first experiments carried out on the TCA Tokamak [1] using Alfvén Wave Heating showed a considerable increase in the radiated power loss during the rf pulse [2,3]. This effect masked the electron heating considerably and the electron temperature increase was maintained only for a few energy confinement times after which it fell to its target plasma value. A program of limiter design and material tests [4] showed that the limiters had been the dominant source of the metallic impurities and we found that narrow carbon limiters gave a better target plasma. More specifically the plasma column resistance and radiated power loss were reduced by a large factor. It was thus considered that the next mostly likely source of metallic impurity influx was the antenna structure.

The original TCA rf antenna system [5] consisted of wide stainless steel plates, in eight groups of three, above and below the plasma. They were unshielded both at their sides and in front for the most recent work [2,3]. The separation between the plasma nominal radius (minimum limiter radius) and the antenna radius was only 20 mm. The total antenna surface represented ~16 % of the plasma surface area. This large area was considered necessary in order to impose fairly pure low n- and m-number spectra on the plasma, avoiding low wavelength parasitic loading effects. We have now removed the original antenna structure and replaced it with new bar antennae. This paper discusses the design of the new antennae, their coupling properties, the changes in target plasma behaviour and finally their performance in higher power heating experiments.

The Design of the Bar Antennae : The requirement that the new antenna system should excite as pure a spectrum of modes as possible was retained. The large poloidal and toroidal extent of each antenna group has been maintained, with even a slight increase in both directions. The mechanical antenna design is shown in Fig. 1. The current distribution in the toroidal direction effectively determines the n-spectrum which is shown in Fig. 2 up to n=26, together with the original wide plates' spectrum. The m-spectrum remains relatively unchanged.

In order to reduce the effects of the edge-plasma, considered to be the main cause of the metallic impurity influx [6], we have increased the antenna-plasma spacing from 20 mm to 30 mm. The antennae are, however, considerably thicker in the radial direction, being constructed out of 10 mm diameter bars. The fact that they have a small "perpendicular" surface area should reduce charge-exchange sputtering, but sputtering due to charged particles attached to the field lines and accelerated by the oscillating electrostatic antenna potential may even increase.

To reduce the quantity and Z of the material sputtered we have coated the steel bars with TiN. This material should have a lower sputtering coefficient, by a large factor, than stainless steel. In addition, the radiated power per impurity atom is less for titanium than for iron, provided the electron temperature is greater than ~600 eV and the coronal equilibrium model is applicable. A layer of 6-7 μm was deposited by Chemical Vapour Deposition by the Laboratoire de Recherche Horlogère (Neuchâtel, Switzerland). A comparison between different methods of TiN deposition was made to determine their sputtering yields [7] and Chemical Vapour Deposition was favoured com-

pared with Physical Vapour Deposition.

The change in antenna design has only slightly modified the antenna electrical characteristics. The value of the antenna inductance has increased from 50 to 60 nH and the vacuum resistance has barely increased. The plasma loading has not changed within the accuracy of the measurement. With the increased plasma-antenna separation we had estimated that the plasma loading could decrease by ~10 % [2]. The fact that the change is less than this may be due to the enhanced coupling of the slightly wider antenna.

Target Plasma and Higher Power rf measurements : We show the plasma performance without the rf pulse, the target plasma conditions, in TABLE I, for the plate antennae and the bar antennae. The generator remained at 2.5 MHz in both cases. We also show the time development of the radiated power profile

TABLE I. Target Plasma Parameters

	PLATE ANTENNAE	BAR ANTENNAE
Series	# 13270	16705 - 18
Gas	D_2	D_2
I_p(kA)	122	130
$n_e(10^{13}\ cm^{-3})$	2.0	2.2
R_{pl} ($\mu\Omega$)	14.2	11
$\beta + li/2$	0.98	0.98
$\int P_{rad}dV$ (kW)	78	55
P_{oh} (kW)	211	186
$\int P_{rad}dV/P_{oh}$	37 %	30 %
$P_{rad}(0)$ (mW cm^{-3})	165	<50
$P_{rad}(0)/\langle P_{rad}\rangle$	83 %	35 %
$P_{rad}(0)/P_{oh}(0)$	9 %	<3 %
$T_i(0)$ (eV)	225	215
$\eta_{metal}(0)$	0.37 %	<0.11 %

for the steel plate antennae and the bar antennae in Fig. 3 a,b). We note that the plasma column resistance has decreased from ~14 to ~11 $\mu\Omega$ as a result of the change. We see from Fig. 3 that the radiated power profile has become more hollow before the rf pulse with a reduction from 165 mW cm^3 to

less than 50 mW cm^3 on axis. The ratio between radiated power and ohmic power on axis is now <3 %. We assume that this radiated power is still mainly due to iron, since the antenna-plasma distance is slightly greater than the minimum antenna-wall distance, and hence calculate a reduction in heavy metal impurity concentration from ~0.37 % to <0.11 %, assuming 0.5 x 10^{-25} W cm^{-3} per electron per ion. The total radiated power has also been reduced.

In Fig. 4 we show the effects of the rf heating pulse (30 msec) compared with the data obtained with the plate antennae [3] under similar conditions. The generator frequency was 2.5 MHz and the excitation structure was (N,M) = (2,1). The increase in resistance has been reduced, as has the increase in radiated power. Spectroscopic measurements have shown a marked reduction in the intensity of the Fe XVIII line, but since we have also observed higher ionisation states, corresponding to higher electron temperatures, no estimate of the iron density reduction factor can be given yet. The most marked change is the larger plasma density increase during the rf pulse. We have generally found a stronger increase following improvements to plasma purity, confirming previous suggestions that this increase cannot be only due to impurity ionisation, but may be fundamental to the presence of the Alfvén wave. During these brief preliminary experiments following the recent antenna change, we have not been able to deliver rf power greater than 80 % of the target plasma ohmic heating power. This may well be related to the greater increase in density.

Conclusions : The new simplified bar antennae have shown good coupling properties in TCA. The removal of the wide steel plates has led to improvements in the target plasma, especially to the radiated power profile. Preliminary heating experiments have shown a stronger increase in the plasma density in addition to a reduced impurity increase.

Acknowledgements : We gratefully acknowledge the help of Ph. Marmillod and the TCA support team in carrying out this work, which was partly supported by the Swiss National Science Foundation.

References.

[1] CHEETHAM A.D. et al., 11th Symp. on Fusion Technology, Oxford, Vol.1,601

[2] de CHAMBRIER A. et al., Plasma Phys. 25 (1983) 1021

[3] BEHN R. et al., Plasma Phys. and Contr. Fus., 26 (1984) 173

[4] BEHN R. et al., Proc. 11th European Conf. on Contr. Fusion and Plasma Physics, Aachen Sept. 1983, Vol 7D, part II, 471

[5] de CHAMBRIER A. et al., Proc. 3rd Joint Varenna-Grenoble Int. Symp., Grenoble. EUR 7979 EN, 1117, 1982

[6] de CHAMBRIER A. et al., invited paper in this conference

[7] C. FERRO and E. FRANCONI, private communication

Figure Captions

Fig. 1: Design of the bar antennae

Fig. 2: n-spectrum of the antennae

Fig. 3a: Radiated power profile for the steel plate antennae

Fig. 3b: Radiated power profile for the bar TiN antennae

Fig. 4: Effects of the rf pulse

NON-LINEAR ANTENNA LOADING MEASUREMENTS IN TCA

A. de Chambrier, G.A. Collins, P.A. Duperrex, M. Grossmann, A. Heym, F. Hofmann, Ch. Hollenstein, B. Joye, R. Keller, A. Lietti, J.B. Lister, F.B. Marcus, J.M. Moret, S. Nowak+, J. O'Rourke*, A. Pochelon, W. Simm

Centre de Recherches en Physique des Plasmas
Association Euratom - Confédération Suisse
Ecole Polytechnique Fédérale de Lausanne
21, Av. des Bains, CH-1007 Lausanne / Switzerland
+ University of Fribourg, Switzerland
* JET-Joint Undertaking, Abingdon, Oxfordshire, OX14 3EA (United Kingdom)

Abstract : The TCA tokamak is mainly dedicated to the study of additional heating by the absorption of Alfvén Waves ($\omega \ll \omega_{ci}$). RF waves are launched by the antennae to heat the plasma core. Unwanted edge dissipation can reduce the heating efficiency and may lead to spurious edge heating. A sufficiently large bias voltage of the antennae can decrease the RF impedance, as well as increase the strength of the wavefields. This observation indicates the presence of some parasitic loading, particularly evident at low power, and reduced above 50 kW. The loading stabilizes at bias voltages below -60 volts. The asymptotic loading is compared with numerically calculated values. The origin of these effects is discussed.

Introduction : The TCA tokamak has been built with the express aim of heating the plasma by Shear Alfvén Waves. Heating power equivalent to the ohmic power has already been delivered by the antennae to the plasma and plasma heating has been observed [1]. The study of coupling RF power from the antennae to the plasma core also involves the question of edge dissipation or losses produced either by the direct field of the antennae or by energy reflected from the plasma. This paper addresses the question of edge parasitic dissipation by applying a polarisation to the antennae. This tool provides an estimate of the part of the energy lost in the edge and suggests modifications to the

antenna structure to improve the core coupling efficiency.

The main TCA parameters are R=61 cm, a=18 cm, $B_\phi \leq 15$ kG and $I_p \leq 175$ kA. The vacuum chamber (SS 316 LN) has a rectangular cross section (average wall radius 27 cm) which allows the poloidal antenna groups (SS 316 LN) to be placed in the free space above and below the plasma [Fig. 1]. There is a pair of antenna groups in each quadrant of the torus and the antenna-plasma spacing is 2 cm. The radial extent of the antenna plates is only 3 mm. The antennae described in the present paper cover 16 % of the total plasma surface and did not possess any lateral screens for most of the measurements reported here. The early measurements in TCA [2,3] were made with such lateral screens. The most commonly used excitation configuration is N=2 M=1 at a frequency of 2.5 MHz.

Each antenna can be polarized with a capacitor bank through a 10 Ω resistance, or left floating. The RF magnetic wavefield is measured with several triple coils placed in ceramic tubes located in the shadow of the limiters.

Polarisation measurements : In the standard shot shown on Fig. 2, the density is ramped by gas-puffing, so as to sweep through the shear Alfvén wave spectrum. As the antennae are individually floating, their floating potential can be measured in an active or passive polarisation experiment. In Fig. 2, the active polarisation is only switched on in the middle of the tokamak discharge. During the current flat-top, all antennae are slightly positive (0-10 volts). When the RF power is applied (here only about 10 kW), all antennae show a drop towards negative potential (t=30 ms). Later on (50 ms), negative polarisation is applied to all antennae, producing a drop in the antennae RF resistance. In the case shown in Fig. 2, some -100 volts of imposed polarisation produce a drop in the antenna RF resistance of some 30 % (full trace). The reference discharge (no polarisation) is also shown (light trace). These resistance drops are particularly marked at low power. Note that in this shot, the initial RF power is about 20 kW, and the RF power and polarisation voltage decay exponentially.

At the same time that the RF impedance drops, surprisingly, the wavefield increases substantially on most of the different magnetic probes, so that even while reducing the transmitted power by applying polarisation (-7 %), the Alfvén modes in the plasma have increased.

This means that the RF antennae impedance can be subdivided into two parts : a useful part which contributes to the wavefields in the plasma

and which improves with negative polarisation, and another part which does not contribute to the wavefields. This parasitic impedance is obviously diminished by applying negative polarisation, because 1) the wavefields increase and furthermore 2) the total emitted power drops. Even though a complete power flow chart has not yet been determined, because the measurement of global wavefield energy relies on local edge magnetic measurements, the qualitative observation of increased antenna efficiency remains.

The edge plasma is also modified due to polarisation : Fig. 2 shows the ion saturation current measured at two points in the scrape-off plasma with a Langmuir probe : top trace at 13 mm from the wall, bottom trace close to the wall, where the density is strongly increased. The tendency is a flattening of the scrape-off density or even a hollowing around the antennae, presumably due to electrostatic particle repulsion, as is shown on Fig. 3. The scrape-off temperature profile is not modified by the polarisation but rather by the RF fields, even at some 10 kW. It is to be noted that neutrals seem to be unaffected by polarisation, as is shown on the D_α-emission measured along a radial chord [Fig. 2].

As the polarisation is increased towards negative values, the RF impedance continues to decrease to a value where it finally saturates. This is shown for different Alfvén resonance conditions for values of the density below the n=-2, m=-1 Discrete Alfvén Wave (DAW) resonance, and above the DAW, where the continuous spectrum begins [Fig. 4].

The decrease of both RF impedance curves stops at some -70 volts on the antennae. The usual value of the sheath potential or of the polarisation acquired by a conductor in a plasma is $V_f(\text{volts}) = 3xT_e(\text{eV})$ for hydrogen and $6xT_e$ for iron. The value of the saturation voltage may therefore be consistent with the measured temperature of 10-12 eV. However, the non Maxwellian nature of the distribution [4] is probably dominant in producing the potential.

The RF impedance reduction at this low level of RF power (10-20 kW) amounts to some 40 % when below the DAW resonance, and to some 30 % when above the resonance, before reaching the asymptotic value. In another series of shots, the RF impedance has been measured as a function of the applied power, Fig. 5a). The impedance reduction is again stronger below the DAW resonance than above (-1 mΩ/kW below, -0.6 mΩ/kW above). This reduction can be explained in a similar way as the results from polarisation experiment, since the antennae are actually negatively polarised by the RF fields interacting with the edge-plasma (-0.8 volts/kW below the DAW, -0.5 volts/kW above), Fig. 5b).

Apart from this DC potential, the antennae are further subject to an important oscillating potential $V_{ant} = \omega L_{ant} I_{ant}$, due to the antenna inductance L_{ant} = 50 nH. This gives about 550 volts (p-p) at 200 kW with the typical value of R_a = 100 m Ω par antenna group.

Early experiments have been made on the antenna system to measure the DC resistance of the antenna plates. This yields information on edge-plasma interactions in the absence of RF. The measurement was made with lateral antenna screens, which protruded 5 mm in front of the antennae in the plasma direction, and which left a 1 cm space on each side of each group of 3 antenna plates [3]. The DC resistance measured in the ion saturation regime is $R_{DC}^{screens}$ = 10 Ω. After removing the screens, this resistance was reduced by an order of magnitude to R_{DC} = 1.2 - 2.5 Ω. This shows the beneficial role of antenna screens in reducing the antenna edge-plasma interaction.

MHD antenna impedance calculation : The measured loading can be compared with a one-dimensional numerical MHD calculation [5]. The results of this calculation are shown in Fig. 5, and compared with low power RF loading measurements, with and without polarisation. The case with polarisation more accurately reflects the general picture of a jump in background loading occuring when crossing the DAW, as obtained in the calculations. The DAW has always been known to be very prominent in high power RF experiments, resulting in a strong reduction of the RF impedance in regions of the spectrum dominated by continuum absorption.

Interpretation and conclusion : The candidates for this additional dissipation are capacitive current between the antennae and the scrape-off plasma. The capacitive coupling between antennae and plasma involves several Debye lengths of the sheath potential drop. The capacitive current has the form $I = \omega C V_{ant} \sim \omega V_{ant} (n_e/T_e)^{1/2}$ and can easily be of the order of the antenna RF current. Conductance (Langmuir) currents similarly increase with increasing electron density and antenna area, but they are minimized in our floating antenna system. Capacitive currents scale with ω^2, explaining why similar antennae working in the ICRH frequency range are fully short-circuited without a full Faraday shield. The negative polarisation induced on the antennae at high power, as well as the increased electron temperature, reduce this additional dissipation, which can represent nearly half of the antenna RF resistance at low power. The effect occurs mainly through particle depletion around the antennae. The suppression of either capacitive or conductance currents requires the use of particle screens.

Acknowledgements : We gratefully acknowledge the help of Ph. Marmillod and the TCA support team in carrying out this work, which was partly supported by the Swiss National Science Foundation.

References :

[1] R. Behn et al., Plasma Physics 26 (1984) 173
[2] A.D. Cheetham, Plasma Physics 24 (1982) 893
[3] A. de Chambrier et al., Heating in tor. plasmas I (1982) 161; III, 1167
[4] A. de Chambrier et al., invited paper at this conf.
[5] K. Appert et al., 11th EPS on Contr. Fus. and Plasma Phys., I (1983), 301

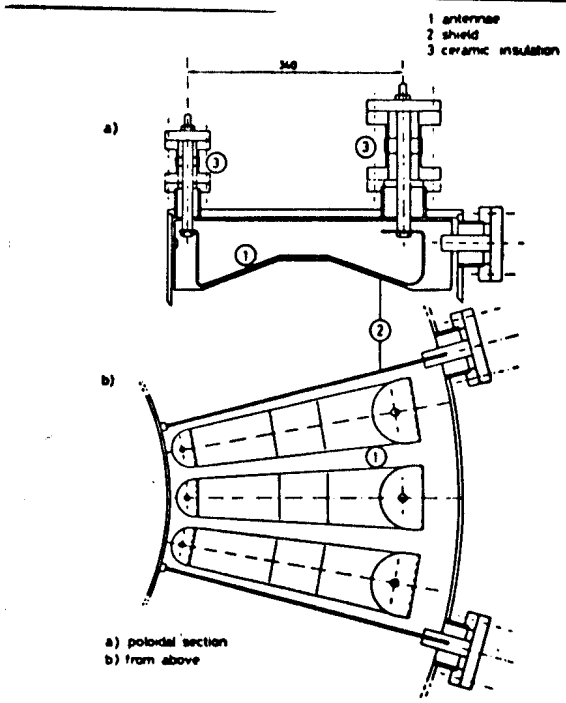

Fig. 1

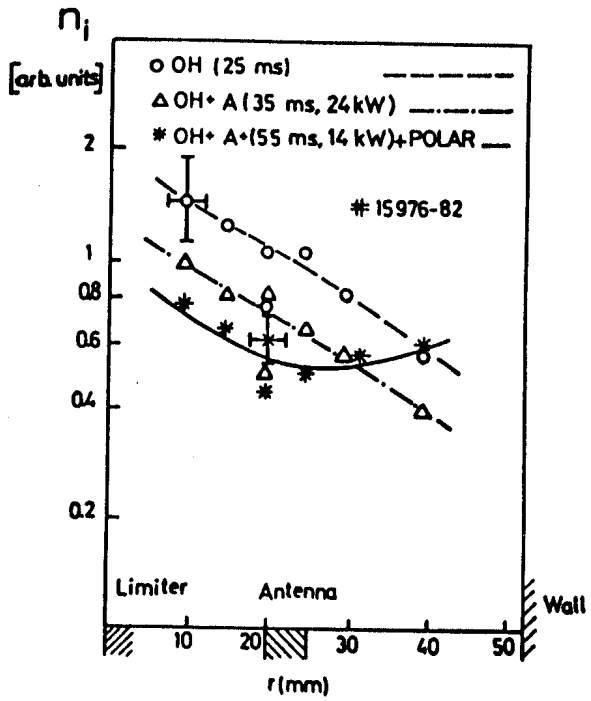

Fig. 3

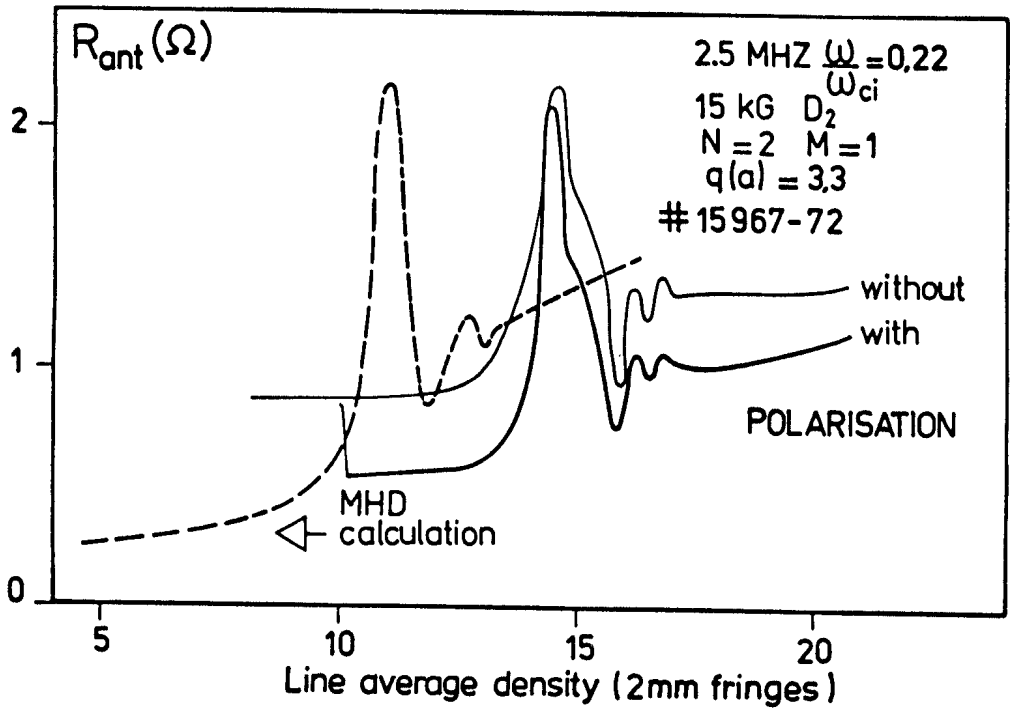

Fig. 5

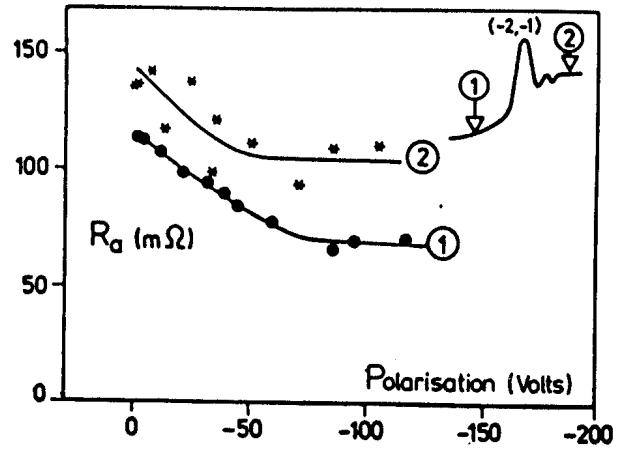

Fig. 4a)

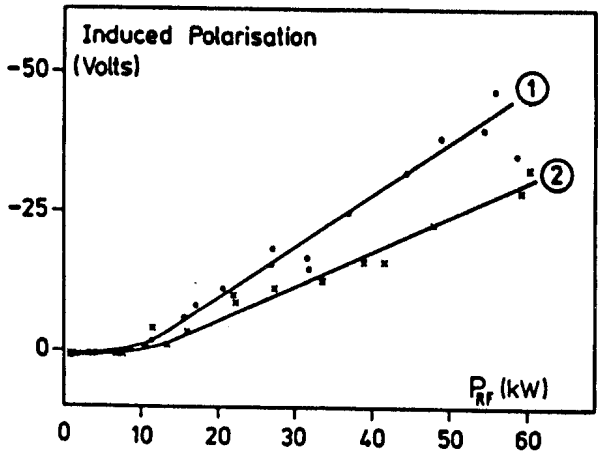

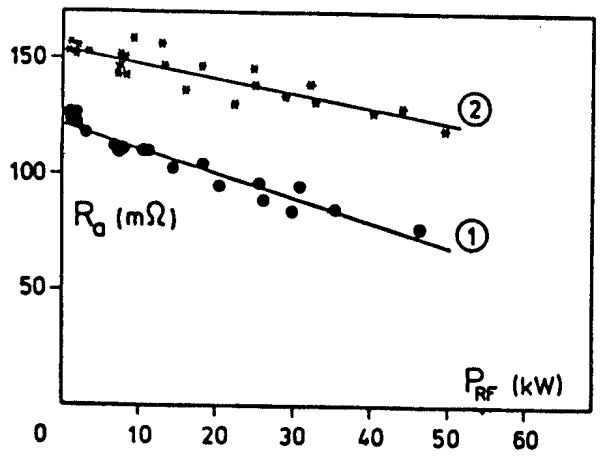

Fig. 4b)

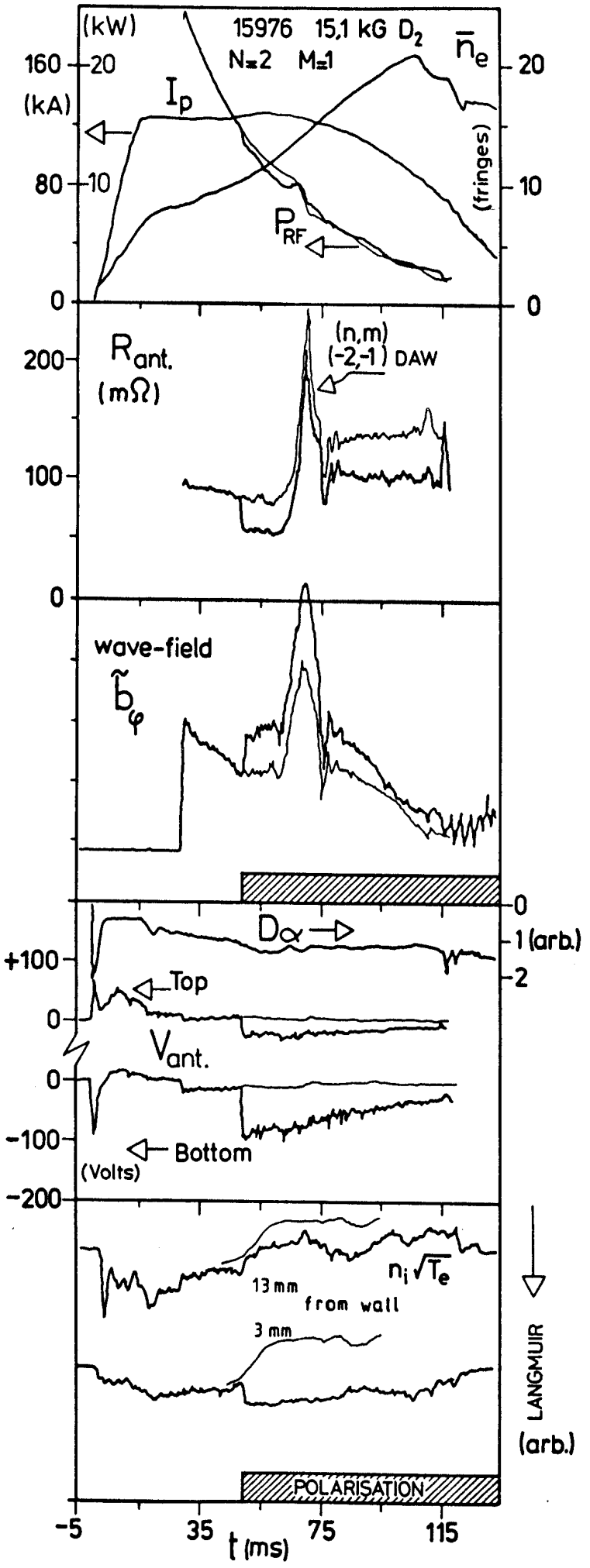

Fig. 2

Paper B17 Non-linear Antenna Loading Measurements in TCA

Keywords :

Tokamak
Radio Frequency Heating
Alfvén Wave Heating
Wavefield
Antenna-plasma interaction
Edge dissipation
TCA
Antenna particle screens

Figures caption :

Fig. 1 Stainless steel plate antennae
Fig. 2 Shot with polarisation (dark trace), and reference discharge (light trace)
Fig. 3 Scrape-off plasma electron density profile
Fig. 4 RF impedance versus polarisation voltage
Fig. 5 a) RF impedance versus polarisation voltage
b) Antennae self polarisation versus RF power
Fig. 6 RF impedance with, without polarisation, compared to MHD calculation.

1 antennae
2 ceramic insulation

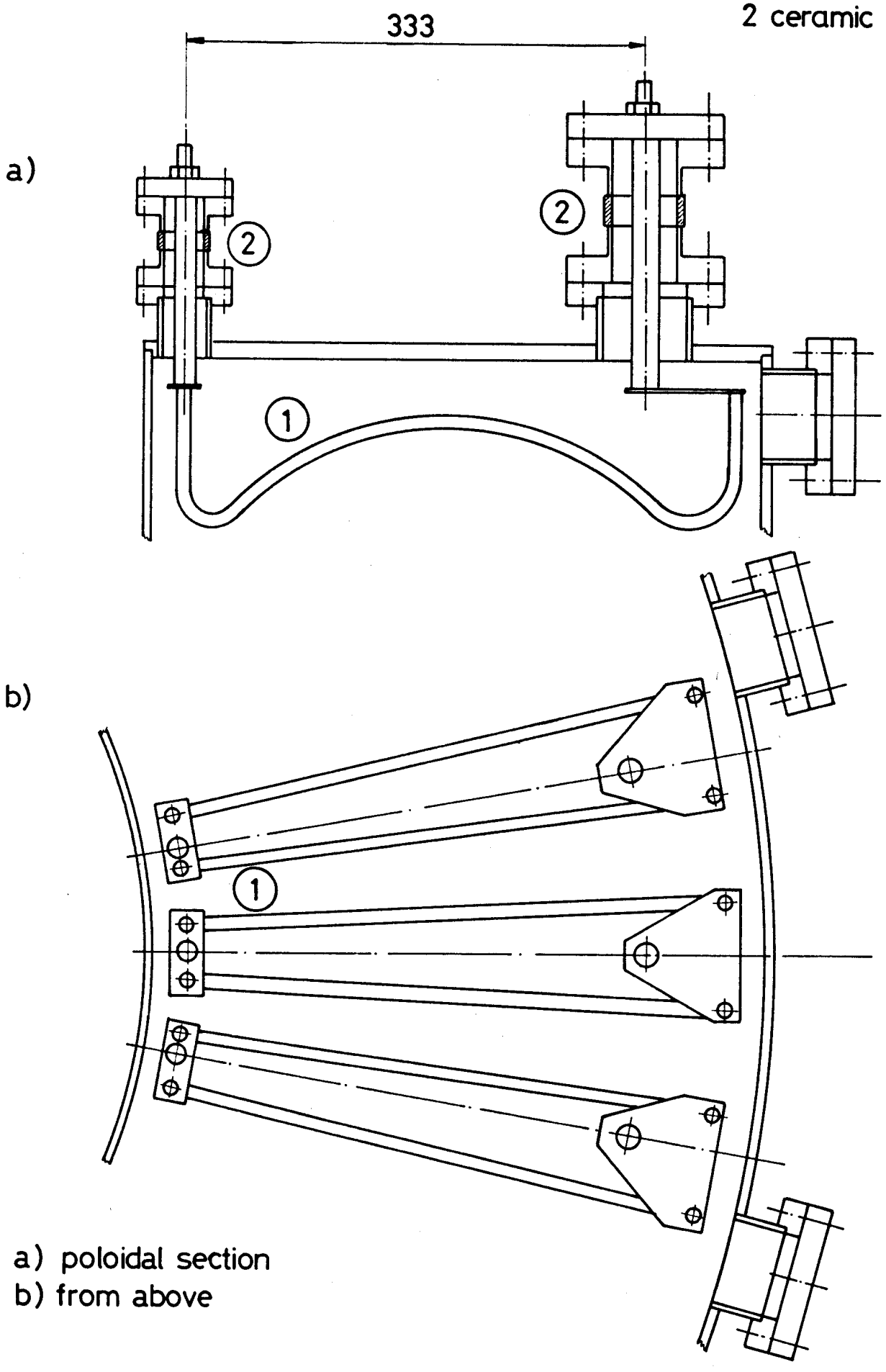

a) poloidal section
b) from above

FIG. 1

FIG. 2

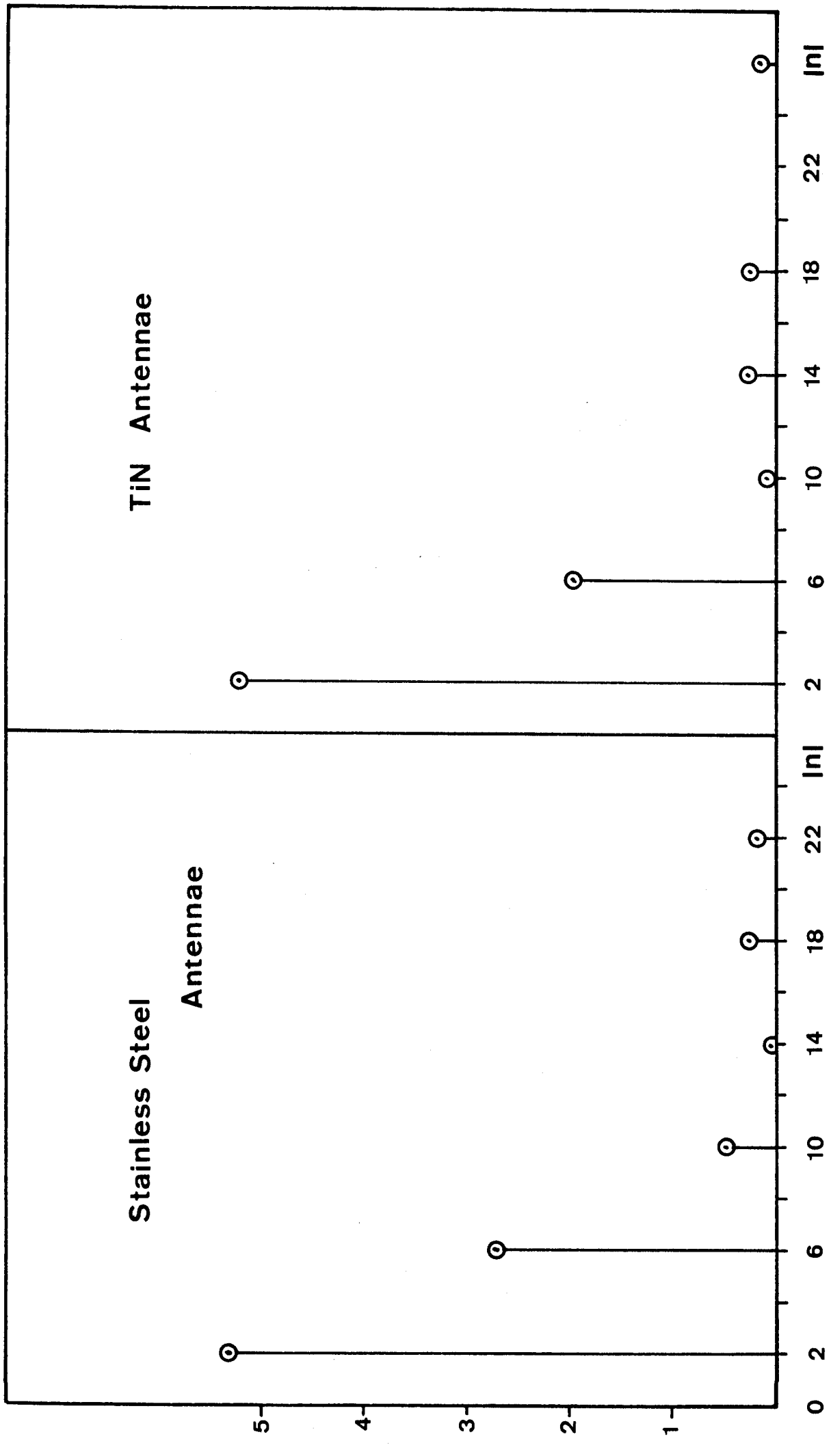
Stainless Steel
Antennae
TiN Antennae
5
4
3
2
1
0
2
6
10
14
18
22
Inl

FIG. 3A

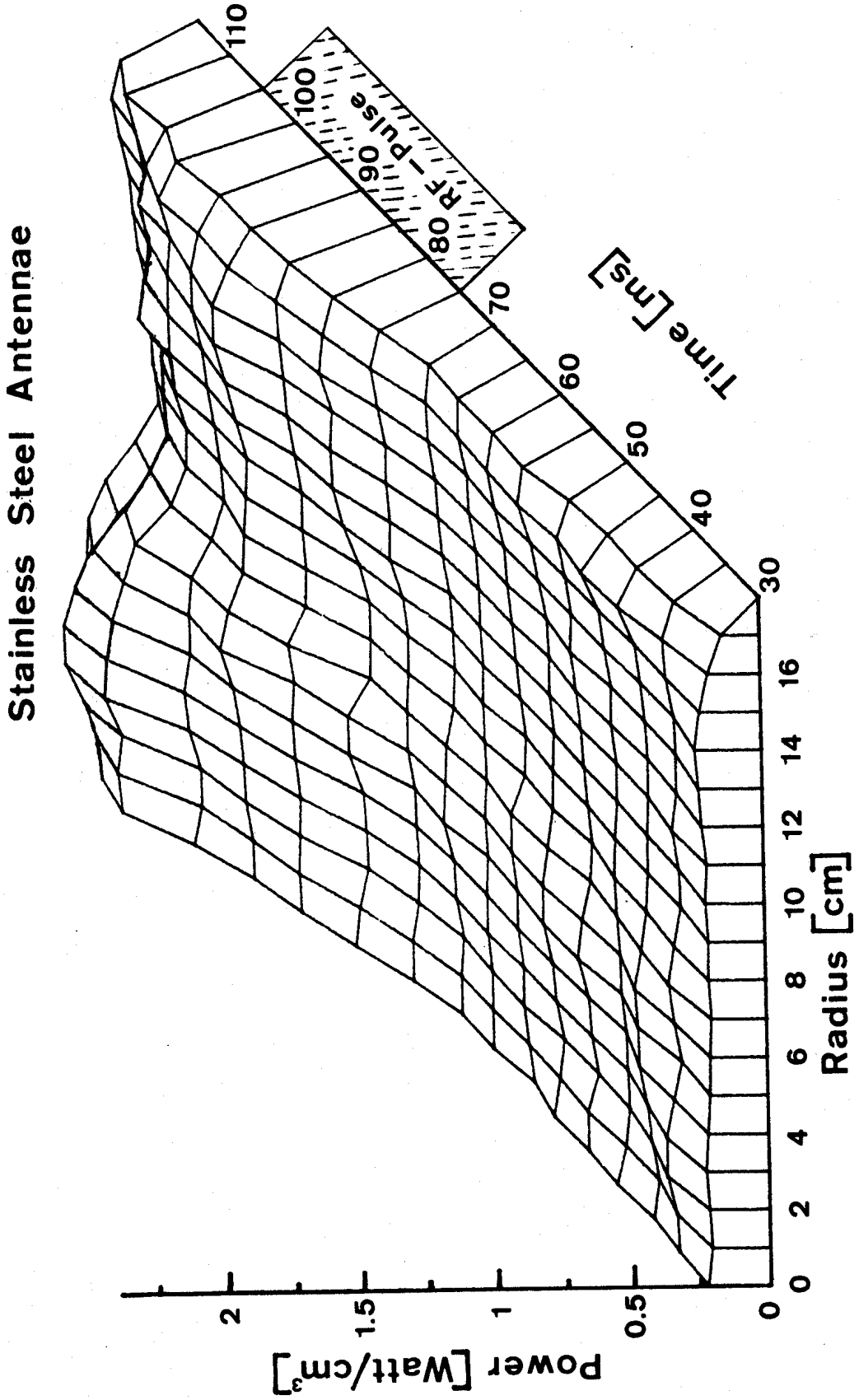
Stainless Steel Antennae
Power [Watt/cm³]
0
0.5
1
1.5
2
Radius [cm]
0
2
4
6
8
10
12
14
16
Time [ms]
30
40
50
60
70
80
90
100
110
RF Pulse

FIG. 3B

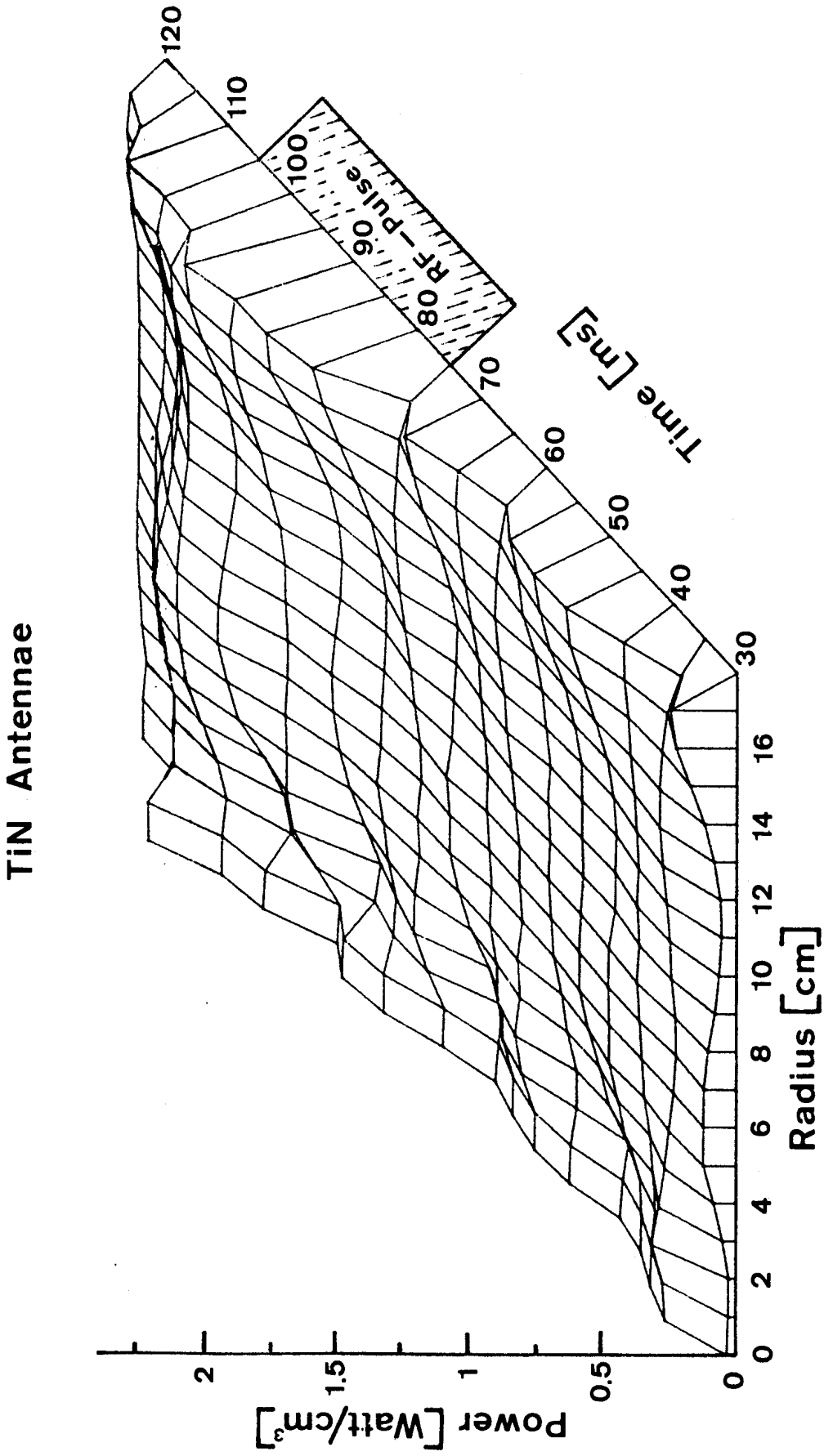
TiN Antennae
Power [Watt/cm³]
0
0.5
1
1.5
2
Radius [cm]
0
2
4
6
8
10
12
14
16
Time [ms]
30
40
50
60
70
80 RF – Pulse
90
100
110
120

FIG. 4

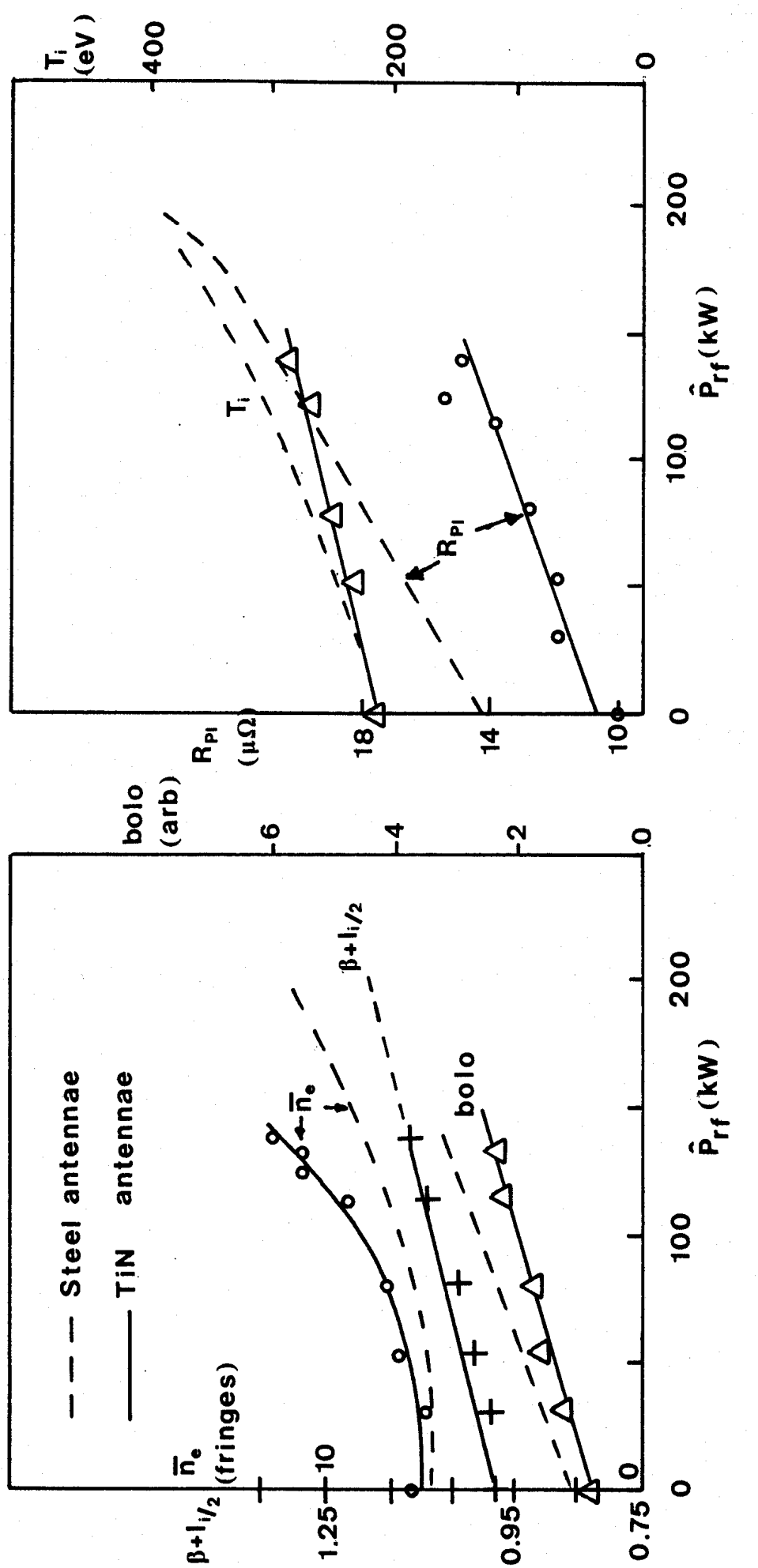
Steel antennae
TiN antennae
$\bar{n}_e$ (fringes)
$\beta+l_i/2$
bolo (arb)
R_{PI} (μΩ)
T_i (eV)
$\hat{P}_{rf}$ (kW)
0.75
0.95
1.25
10
0
100
200
400
18
14
10
2
4
6